A Dual-Function MIMO Radar-Communication System Via Waveform Permutation

Aboulnasr Hassanien, Elias Aboutanios, Moeness G. Amin, Giuseppe A. Fabrizio

Abstract

Cooperative transmissions for radar and communication tasks have been recently studied with the goal of addressing the problem of the increasingly crowded RF spectrum. In this paper, we propose a dual-function radar communication (DFRC) system in which the radar platform and resources are used for target probing and communication symbol embedding simultaneously. The proposed DFRC system is based on the concept of multiple-input multiple-output (MIMO) in tandem with transmit beamforming where a number of transmit beams, which can be larger than the number of transmit antennas, are formed. We show that the transmit beamforming weight vectors may be designed to achieve transmit processing gain, embed communication symbols intended for the communication receiver, and prevent eavesdroppers from intercepting the communication message. Our proposed method for embedding communication symbols into the MIMO radar emissions is based on changing the order of the orthogonal waveforms along the transmit beams from one pulse repetition period to another. In so doing, the communication symbols are represented by different associations of the orthogonal radar waveforms and transmit beams. We show that the data rate is proportional to the factorial of the number of transmit beams, which permits high data rates (in the megabits per second) for a moderate number of transmit antennas. The error probability is analyzed and the bounds on the symbol error rate are derived. We show that changing the number of transmit beams leads to a tradeoff between the data rate and target detection accuracy. Simulation examples are provided for performance evaluation and to demonstrate the effectiveness of the proposed information embedding technique.

Index Terms

MIMO radar, dual-function radar communications, shared-spectrum access, bit error rate.

A. Hassanien is with the Dept. of Electrical Engineering, Wright State University, Dayton, OH 45435, USA. E. Aboutanios is with the School of Elec. Eng. and Telecomm., UNSW Australia, Sydney Australia. M. G. Amin is with the Center for Advanced Communications, Villanova University, Villanova, PA, USA. G. A. Fabrizio is with the Defence Science and Technology Group, Edinburgh, SA 5111, Australia. (emails: hassanien@ieee.org; elias@ieee.org; moeness.amin@villanova.edu; joe.fabrizio@dsto.defence.gov.au).

I. Introduction

Co-existence between radar and communications can take different forms and employ various strategies [1]–[5]. The two systems can be deployed using separate platforms [6]–[13] or may have a common transmitter. In both cases, joint waveform design is likely to proceed to minimize mutual interference when operating in the same frequency band. Furthermore, if a cooperative transmitter is employed for both systems, the radar resources, including power, bandwidth, aperture, and RF front ends, can be put at the disposal of the communication signaling task, provided that the radar primary function is compromised as little as possible [14], [15].

Towards minimizing the mutual interference between the radar and communication signals, communication symbols can be embedded into the radar emissions [16], which defines what is known as dual-function radar-communication (DFRC) systems [17]–[23]. These systems may modulate the radar beam [24] or the radar waveform [20], [25], or both. Communication signal embedding is performed over each pulse repetition interval (PRI) and can employ different modulation schemes including amplitude shift-keying and phase-shift keying (PSK). A number of variants of DFRC systems have been recently introduced. For example, changes in sidelobe levels, achieved by designing multiple beam patterns with a shared common mainlobe, permit the transmission of different symbols towards a designated user [24]. It was shown in [22], [26], [27] that synthesizing the radar pulse by orthogonal waveforms in a multiple-input single-output system allows waveform diversity to play a fundamental role in embedding phase modulated signals in radar emissions. Information embedding can also be achieved by modulating the radar waveform in fast time [20], [28].

In this paper, we consider MIMO DFRC systems where signal embedding benefits from the multi-sensor radar aperture and capitalizes on the available orthogonal or weakly correlated waveforms imposed by the MIMO radar operation. The main goal is to use the radar's original waveforms in place of the composite radar-communication waveforms, and as such, avoid joint waveform design that may disadvantage the primary radar functionality and reduce its power. At the core of our contribution is to dually allocate the available power for both radar and communications not without any reduction in the radar power. This provides high SNR and subsequently increases the communication bit rate. We accomplish this goal by embedding communication symbols through the shuffling of the independent waveforms across the transmit antennas. This means each communication symbol corresponds to one particular order of the

waveforms along the aperture. Waveform shuffling is transparent to the radar operation and does not change the radar receiver performance or compromise the offerings of the MIMO radar. In essence, since permutations used to shuffle the waveforms are known to the radar, the unshuffling at the radar receiver amounts to undoing the permutations at the transmitter and reassigning the waveforms to their reference antennas. This operation restores the coherent structure of the MIMO radar data, enabling the radar functionality to proceed as in the case of unshared platform and independent functions. In this respect, the only burden placed on the DFRC system is the additional complexity associated with applying the permutation operation during the transmit mode and reversing the permutation during the radar receive mode.

We derive the achievable data rate under the proposed signaling scheme and show that the number of symbols that can be embedded is a factorial of the number of transmit antennas. Toward this end, the large number of degrees of freedom that are available in choosing symbol combinations is exploited for the lowest possible symbol error rate (SER). The latter is investigated as a function of signal-to-noise ratio (SNR) and the direction of the communication receiver.

The paper is organized as follows. Section II presents the MIMO radar signal model. Section III describes the proposed information embedding scheme whereas section IV discusses beamforming design techniques for DFRC systems. Section V gives some performance analysis. Simulation results are given in section VI and conclusions are drawn in section VII.

II. MIMO Radar Signal Model

Consider a joint radar-communication system that embeds information into the radar emissions as a secondary function. The system consists of a dual-function MIMO radar platform and a communication receiver, as illustrated in Fig. 1. The MIMO radar platform is equipped with a dual-function transmit array comprising M omnidirectional colocated transmit antennas and a receive array of N colocated antennas arranged in an arbitrary linear shape. Without loss of generality, we assumed that the transmit array is a uniform linear array (ULA) with inter-element spacing d measured in wavelength. It is also assumed that both the transmit and receive arrays are located in close proximity to one another such that a target in the far-field would be seen from the same direction by both arrays.

Let $\mathbf{\Phi}(t) = [\phi_1(t), \ldots, \phi_K(t)]^T$ be the $K \times 1$ vector of transmit waveforms where $(\cdot)^T$ denotes matrix transpose and $\{\phi_k(t)\},\ k = 1, \ldots, K$, is a pre-designed set of orthogonal waveforms. The

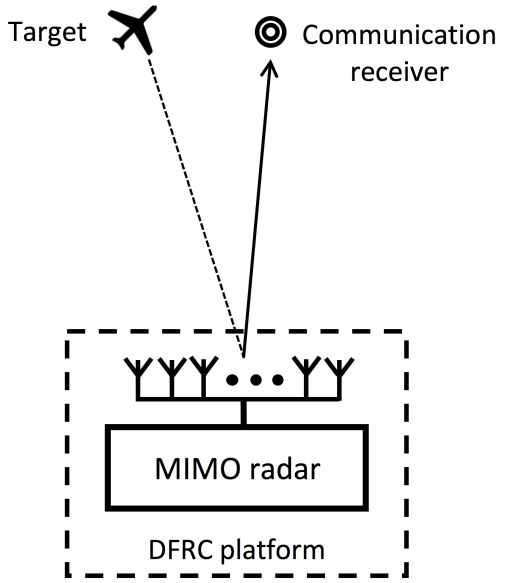

Fig. 1. Illustrative diagram of a joint MIMO radar and communication system

orthogonal transmit waveforms satisfy the condition

$$\int_{T_0} \phi_k(t)\phi_{k'}^*(t)dt = \delta(k-k'), \tag{1}$$

where t is the fast time index, T_0 is the radar pulse width, $(\cdot)^*$ denotes the conjugate, and $\delta(\cdot)$ is the Kronecker delta function.

Transmit beamforming techniques are used in MIMO radar to achieve transmit coherent processing gain. Let $\mathbf{\Theta} = [\theta_{\mathtt{min}},\ \theta_{\mathtt{max}}]$ be the spatial sector where the radar operation takes place, i.e., where the transmit energy should be focused, and $\mathbf{w}_k$ be the $M \times 1$ weight vector used to form a transmit beam to focus the k^{th} waveform $\phi_k(t)$ within the desired spatial sector $\mathbf{\Theta}$. Using K transmit beamforming weight vectors $\mathbf{w}_k,\ k = 1, \ldots, K$, the baseband representation of the $M \times 1$ transmit signal vector $\mathbf{s}_a(t)$ can be expressed as a linear combination of the individual orthogonal waveforms, i.e.,

$$\mathbf{s}_a(t) = \sum_{k=1}^{K} \mathbf{w}_k^* \phi_k(t) = \mathbf{W}^* \mathbf{\Phi}(t), \tag{2}$$

where $\mathbf{W} = [\mathbf{w}_1, \ldots, \mathbf{w}_K]$ is the $M \times K$ transmit beamforming weight matrix. Note that the transmit energy per pulse is normalized to unity. We assume that the total transmit energy in a single pulse is fixed to $E_t = M$. This can be satisfied by normalizing the weight matrix $\mathbf{W}$ such that $\mathrm{tr}\{\mathbf{W}^H\mathbf{W}\} = M$, where $\mathrm{tr}\{\cdot\}$ denotes the trace of a square matrix. It is worth

noting that $\mathbf{s}_a(t)$ is the vector of the baseband signals used at the transmit side of the MIMO radar system. From a practical viewpoint, transmit power efficiency is achieved by employing constant modulus signals. It is noted, however, that from a receiver perspective, the signal model (2) enables pulse compression using the signal vector $\mathbf{\Phi}(t)$ which need not be constant modulus. This permits additional degrees of freedom in designing the individual orthogonal waveforms.

Considering Q point targets in the far-field, the $N \times 1$ complex vector of the received observations can be expressed as [29]

$$\begin{aligned}\mathbf{x}\left(t,\tau\right) &= \sum_{q=1}^{Q} \beta_q\left(\tau\right)\left[\mathbf{a}^T\left(\theta_q\right)\mathbf{s}_a(t)\right]\mathbf{b}\left(\theta_q\right) + \mathbf{n}\left(t,\tau\right) \\ &= \sum_{q=1}^{Q} \beta_q\left(\tau\right)\left[\left(\mathbf{W}^H\mathbf{a}(\theta_q)\right)^T\mathbf{\Phi}(t)\right]\mathbf{b}\left(\theta_q\right) + \mathbf{n}\left(t,\tau\right) \end{aligned} \tag{3}$$

where τ is the pulse number, $\beta_q\left(\tau\right)$ is the reflection coefficient of the q^{th} target, θ_q is the spatial angle associated with the q^{th} target, $\mathbf{a}\left(\theta\right)$ and $\mathbf{b}\left(\theta\right)$ are the steering vectors of the transmit and receive arrays, respectively, $(\cdot)^H$ stands for the Hermitian transpose, and $\mathbf{n}\left(t,\tau\right)$ is the $N \times 1$ vector of zero-mean white Gaussian noise. In (3), the reflection coefficients $\beta_q\left(\tau\right),\ q = 1,\ldots,Q$ are assumed to obey the Swerling II target model [30].

Matched-filtering is applied at the radar receiver to extract the received signal components associated with the individual transmitted waveforms. Assuming that the K transmit waveforms satisfy the orthogonality condition at all time-delays and Doppler-shifts within the range and velocity specifications of the radar, matched-filtering the received data to the waveforms yields the $KN \times 1$ extended virtual data vector

$$\begin{aligned}\mathbf{y}(\tau) &= \mathrm{vec}\left(\int_{T_0}\mathbf{x}(t,\tau)\mathbf{\Phi}^H\left(t\right)dt\right) \\ &= \sum_{q=1}^{Q}\beta_q(\tau)\left[\left(\mathbf{W}^H\mathbf{a}(\theta_q)\right)\otimes\mathbf{b}\left(\theta_q\right)\right] + \tilde{\mathbf{n}}\left(\tau\right), \end{aligned} \tag{4}$$

where the operator $\mathrm{vec}\left(\cdot\right)$ stacks the columns of a matrix into a single column vector, $\otimes$ denotes the Kronecker product, and

$$\tilde{\mathbf{n}}(\tau) = \mathrm{vec}\left(\int_{T_0}\mathbf{n}(t,\tau)\mathbf{\Phi}^H(t)dt\right) \tag{5}$$

is the $KN \times 1$ noise term with covariance given by $\sigma_z^2\mathbf{I}_{KN}$ where $\mathbf{I}_{KN}$ denotes the identity matrix of size $KN \times KN$. In practice, perfectly orthogonal waveforms with overlapped spectral contents cannot be achieved, and consequently waveforms with low cross-correlations should be

used. The problem of waveform design with low cross-correlations has been extensively studied in the literature (see [31], [32], and references therein).

III. Proposed Formulation and Information Embedding Scheme

In this section, we show that MIMO radar with transmit beamforming and waveform permutation yields the same extended virtual array model at the radar receiver. This section also presents the proposed information embedding scheme based on shuffling the transmit MIMO radar waveforms.

A. MIMO Radar With Waveform Permutation

Let $\mathbf{P}$ be an $K \times K$ arbitrary permutation matrix. Applying the permutation to the vector of waveforms $\mathbf{\Phi}(t)$ yields the $K \times 1$ vector of shuffled waveforms $\mathbf{\Psi}(t)$, that is

$$\mathbf{\Psi}(t) = \mathbf{P}\mathbf{\Phi}(t). \tag{6}$$

Using the permutation matrix properties $\mathbf{P}^H = \mathbf{P}^T$ and $\mathbf{P}^{-1} = \mathbf{P}^T$, we have

$$\begin{aligned}\mathbf{\Psi}(t)\mathbf{\Psi}^H(t) &= \mathbf{P}\mathbf{\Phi}(t)\mathbf{\Phi}^H(t)\mathbf{P}^H \\ &= \mathbf{P}\mathbf{P}^T = \mathbf{I}_K.\end{aligned} \tag{7}$$

Therefore, the shuffling operation does not affect the orthogonality between different waveforms. By using the vector of shuffled orthogonal waveforms $\mathbf{\Psi}(t)$ at the MIMO radar transmitter, the $N \times 1$ complex vector of the radar received observations can be rewritten as

$$\tilde{\mathbf{x}}(t,\tau) = \sum_{q=1}^{Q} \beta_q(\tau) \left[\left(\mathbf{W}^H \mathbf{a}(\theta_q) \right)^T \mathbf{\Psi}(t) \right] \mathbf{b}\left(\theta_q\right) + \mathbf{n}\left(t,\tau\right). \tag{8}$$

Since the shuffling is known at the radar receiver, matched-filtering the data (8) to the permuted vector of orthogonal waveform $\mathbf{\Psi}(t)$ yields

$$\begin{aligned}\tilde{\mathbf{y}}(\tau) &= \mathrm{vec}\left(\int_{T_0} \tilde{\mathbf{x}}(t,\tau)\mathbf{\Psi}^H(t)dt \right) \\ &= \sum_{q=1}^{Q} \beta_q\left(\tau\right) \left[\left(\mathbf{W}^H \mathbf{a}(\theta_q) \right)^T \otimes \mathbf{b}\left(\theta_q\right) \right] + \breve{\mathbf{n}}(\tau),\end{aligned} \tag{9}$$

where

$$\begin{aligned}\breve{\mathbf{n}}(\tau) &= \mathrm{vec}\left(\int_{T_0} \mathbf{n}(t,\tau)\mathbf{\Psi}^H(t)dt \right) \\ &= \mathrm{vec}\left(\left[\int_{T_0} \mathbf{n}(t,\tau)\mathbf{\Phi}^H(t)dt \right] \mathbf{P}^T \right)\end{aligned} \tag{10}$$

is the $KN \times 1$ additive noise term with covariance $\sigma_n^2 \mathbf{I}_{KN}$.

By comparing the virtual signal models (4) and (9), we see that the MIMO radar with and without waveform permutation yields the same data model at the radar receiver except for a permutation on the additive noise term. In this respect, following the waveform shuffling, the noise term in (10) can be expressed in terms of the noise term (5) using the following relationship

$$\breve{\mathbf{n}}(\tau) = [\mathbf{P} \otimes \mathbf{I}_N]\tilde{\mathbf{n}}(\tau). \tag{11}$$

Both $\breve{\mathbf{n}}(\tau)$ and $\tilde{\mathbf{n}}(\tau)$ are zero-mean white Gaussian noise with covariance $\sigma_n^2 \mathbf{I}_{KN}$. This implies that using a permuted version of the orthogonal waveforms at the input of the transmit array does not alter the MIMO radar operation.

B. Information Embedding Using Waveform Permutation

In MIMO radar with transmit beamforming, each column of the transmit beamforming weight matrix $\mathbf{W}$ is used to form a transmit beam. Therefore, during each radar pulse, K beams are simultaneously formed. The beampattern associated with each beam is defined as

$$g_k(\theta) = \left\| \mathbf{w}_k^H \mathbf{a}(\theta) \right\|^2, \qquad \theta \in \left[-\frac{\pi}{2}, \frac{\pi}{2} \right), \ k = 1, \ldots, K. \tag{12}$$

Let $\mathcal{S} = \{\phi_1(t), \ldots, \phi_K(t)\}$ be the set of orthogonal waveforms. During each radar pulse, all K waveforms are transmitted simultaneously; one waveform via each beam. Therefore, the assignment of K orthogonal waveforms to the K transmit beams is essentially a permutation of the elements of $\mathcal{S}$. Let us denote the possible permutations as $\mathcal{S}_\ell$ for $\ell = 1, \ldots, L_{\text{perm}}$, where $\mathcal{S}_1 \triangleq \mathcal{S}$ is the reference arrangement, $L_{\text{perm}} = K!$ is the total number of permutations, and $(\cdot)!$ represents the factorial of a non-negative number. A permutation $\mathcal{S}_\ell$ on $\mathcal{S}$ can be expressed in terms of the corresponding $K \times K$ permutation matrix $\mathbf{P}_\ell$. Thus, the ℓ^{th} vector of permuted waveforms is obtained from the original vector of orthogonal transmit waveforms $\mathbf{\Phi}(t)$ as

$$\mathbf{\Psi}_\ell(t) = \mathbf{P}_\ell \mathbf{\Phi}(t), \quad \ell = 1, \ldots, L_{\text{perm}}. \tag{13}$$

To embed information into the MIMO radar emission, we employ the vectors of permuted waveforms as communication symbols. That is, during each PRI, one of the permuted waveform vectors is drawn and transmitted based on the communication message being embedded. In essence, each permutation matrix corresponds to one communication symbol. Suppose that during the τ^{th} radar pulse, the transmit set of waveforms is $\mathbf{\Psi}(t;\tau) \in \{\mathbf{\Psi}_1(t), \ldots, \mathbf{\Psi}_{L_{\text{perm}}}(t)\}$ and assume

that the communication user knows its direction θ_c relative to the stationary MIMO transmit platform. Then, the baseband representation of the signal at the input of the communication receiver is modeled as

$$\begin{aligned} r_{\rm com}(t;\tau) &= \alpha_{\rm ch}\Big(\mathbf{W}^H\mathbf{a}(\theta_c)\Big)^T\mathbf{\Psi}_\ell(t) + z(t;\tau) \\ &= \alpha_{\rm ch}\Big(\mathbf{W}^H\mathbf{a}(\theta_c)\Big)^T\mathbf{P}(\tau)\mathbf{\Phi}(t) + z(t;\tau), \end{aligned} \tag{14}$$

where $\alpha_{\rm ch}$ is the channel coefficient representing the propagation environment between the MIMO radar transmit array and the communication receiver, and $z(t;\tau)$ is noise additive term which is assumed to be Gaussian with mean zero and variance σ_z^2.

The communication receiver has perfect knowledge of the vector of orthogonal waveforms $\mathbf{\Phi}(t)$. Matched-filtering the received data (14) to $\mathbf{\Phi}(t)$ yields

$$\begin{aligned} \mathbf{r}_{\rm com}(\tau) &= \text{vec}\left(\int_{T_0} r(t;\tau)\mathbf{\Phi}^H(t)dt\right) \\ &= \alpha_{\rm ch}\mathbf{P}^T(\tau)\mathbf{W}^H\mathbf{a}(\theta_c) + \mathbf{z}(\tau) \\ &= \alpha_{\rm ch}\mathbf{s}_{\rm com}(\tau) + \mathbf{z}(\tau), \end{aligned} \tag{15}$$

where $\mathbf{z}(\tau) = \text{vec}\left(\int_{T_0} z(t;\tau)\mathbf{\Phi}^H(t)dt\right)$ is the vector of zero-mean additive white noise with covariance $\sigma_z^2\mathbf{I}_K$, and

$$\mathbf{s}_{\rm com}(\tau) \triangleq \mathbf{P}^T(\tau)\mathbf{W}^H\mathbf{a}(\theta_c) \tag{16}$$

is the $K \times 1$ vector of received communication symbol. Define the $K \times 1$ transmit beamspace steering vector as

$$\mathbf{a}_{\rm BS}(\theta) = \mathbf{W}^H\mathbf{a}(\theta). \tag{17}$$

Equations (16) and (17) show that the communication receiver signal at the output of the matched-filter is a (scaled and noisy) permutation of the transmit beamspace steering vector towards the intended communication direction, i.e., a permutation of $\mathbf{a}_{\rm BS}(\theta_c)$. Therefore, the permutation matrix $\mathbf{P}(\tau)$ can be recovered from the received vector $\mathbf{r}_{\rm com}(\tau)$ by determining the permuted elements of the steering vector $\mathbf{a}_{\rm BS}(\theta_c)$ provided that they are distinct.

Assume that L ($L \leq L_{\rm perm}$) distinct permutation matrices are appropriately selected to form the dictionary $\mathbb{D}_{\rm P} = \{\mathbf{P}_1, \ldots, \mathbf{P}_L\}$. Information embedding at the transmit side is achieved by selecting the vector of transmit signals such that $\mathbf{P}(\tau) \in \mathbb{D}_{\rm P}$. Using (16), the corresponding

dictionary of distinct communication symbols at the communication receiver can be constructed as

$$\mathbb{D}_{\rm s} = \{\mathbf{s}_1(\theta_c), \ldots, \mathbf{s}_L(\theta_c)\}\,. \tag{18}$$

Thus, during a particular radar pulse, the embedded communication symbol can be detected by comparing $\mathbf{s}_{\rm com}(\tau)$ to the symbols in $\mathbb{D}_{\rm s}$, as explained in the following subsection. The cardinality L of the dictionary is directly related to the data radar performance while $L_{\rm perm}$ determines the capacity of the communication system as discussed in section V.

At this point, two remarks are in order:

Remark 1: The communication receiver is able to recognize the transmitted symbol provided its elements are distinct. Since the transmitted symbol at the receiver is a permutation of the steering vector, which is a function of the direction of the communication receiver with respect to the radar, we expect that the communication receiver's ability to detect the embedded symbol would depend on the direction at which the receiver is located. This will be discussed in more details in Sec. V.

Remark 2: The MIMO radar receiver has perfect knowledge of the vector of permuted waveforms $\mathbf{\Psi}_\ell(t)$ and, consequently, it is able to apply the correct matched-filters to undo the shuffling, as explained earlier in Sec. III-A. Therefore, the act of embedding communication symbols into the radar signal does not impact the radar's primary tasks, whether they pertain to target detection, direction-of-arrival estimation, tracking, or otherwise.

C. Received Symbol Detection

Let us assume for the purpose of this work that the channel is non-changing and has unity gain[1]. Since the noise follows a multivariate complex Gaussian distribution with zero mean and covariance matrix $\sigma_z^2\mathbf{I}_K$, the pdf of $\mathbf{r}_{\rm com}(\tau)$ is given by

$$\begin{aligned} f\left(\mathbf{r}_{\rm com}(\tau)\big|\mathbf{s}_{\rm com}(\tau)\right) &= \frac{1}{\left(\pi\sigma_z^2\right)^M}\exp\left\{-\frac{\left\|\mathbf{r}_{\rm com}(\tau)-\alpha\mathbf{P}^T(\tau)\mathbf{a}_{\rm BS}(\theta_c)\right\|^2}{\sigma_z^2}\right\} \\ &= \frac{1}{\left(\pi\sigma_z^2\right)^M}\exp\left\{-\frac{\left\|\mathbf{r}_{\rm com}(\tau)-\alpha\mathbf{s}_{\rm com}(\tau)\right\|^2}{\sigma_z^2}\right\}, \end{aligned} \tag{19}$$

[1]In practice, we assume that the channel is estimated accurately. Training sequences can be periodically transmitted to update the channel estimate.

where α is an unknown complex scalar. The maximum likelihood detector then becomes

$$\hat{\mathbf{s}}_{\rm com}(\tau) = \arg \min_{\alpha, \mathbf{s} \in \mathbb{D}_s} \left\| \mathbf{r}_{\rm com}(\tau) - \alpha \mathbf{s} \right\|^2 . \tag{20}$$

This is equivalent to finding the permutation matrix $\mathbf{P}$ such that

$$\hat{\mathbf{P}}(\tau) = \arg \min_{\mathbf{P}} \left\| \mathbf{r}_{\rm com}(\tau) - \mathbf{P}^T \mathbf{a}_{\rm BS}(\theta_c) \right\|^2 . \tag{21}$$

Writing the minimization in terms of the permutation matrix ensures that the properties of the permutation are expressed in the detector. This minimization, however, is not a simple problem and its implementation in the general case is beyond the scope of this work. For small values of M, we can enumerate the symbols $\mathbf{s}_\ell(\theta_c)$, and an exhaustive search can be used to implement the detector. We employ this approach for the purpose of illustration in this paper.

IV. Transmit Beamforming Design for DFRC with Robustness Against Eavesdropping

In this section, we develop a method for transmit beamforming design for joint MIMO radar and communication systems. In the context of MIMO radar, transmit beamforming has been used to achieve transmit coherent processing gain by focusing the transmit energy within certain desired spatial sector(s). Here, we propose to additionally employ transmit beamforming to enforce a certain structure to the transmit beamspace steering vector towards the intended communication direction. Furthermore, transmit beamforming can be appropriately designed to provide robustness against eavesdropping.

As we discussed in the previous sections, the permuted versions of the transmit beamspace steering vector $\mathbf{a}_{\rm BS}(\theta_c)$ are used as communication symbols. To enhance the probability of detection, we need to ensure that all symbols in the dictionary are unique and detectable with equal probability. This can be achieved by restricting the phases of the entries of $\mathbf{a}_{\rm BS}(\theta_c)$ to be uniformly distributed on the unit circle, which is expressed through the following equality constraint

$$\begin{aligned} \angle \mathbf{a}_{\rm BS}(\theta_c) &= \angle \mathbf{W}^H \mathbf{a}(\theta_c) \\ &= \left[0, \ \frac{2\pi}{K}, \ldots, \ (K-1)\frac{2\pi}{K} \right]^T , \end{aligned} \tag{22}$$

where $\angle\cdot$ denotes the angle of a complex number. Additionally, robustness against an eavesdropper located at direction θ_e can be assured by enforcing all transmit beams to have the same phase towards the eavesdropper direction, that is,

$$\angle \mathbf{w}_1^H \mathbf{a}(\theta_e) = \cdots = \angle \mathbf{w}_K^H \mathbf{a}(\theta_e). \tag{23}$$

Convex optimization based techniques can be used to design the transmit beamforming weight matrix $\mathbf{W}$ while satisfying the phase conditions (22) and (23). For the remainder of this paper, we assume that the matrix $\mathbf{W}$ is appropriately designed.

V. Performance Analysis

Now, we turn to the proposed communication scheme. We first establish the maximum achievable bit rate. Then, we discuss the dependence of the channel on the spatial angle of the communication receiver with respect to the transmitter and describe a simple strategy for mitigating this dependence. Finally, we establish an upper bound on the symbol error rate.

A. Conventional MIMO Radar Case

In this subsection, we analyze the theoretical performance of the DFRC system when the radar operates in conventional MIMO radar mode. This is a special case of (3) obtained by putting $\mathbf{W} = \mathbf{I}_M$ resulting in the virtual transmit steering vector being identical to the actual transmit array steering vector, that is, $\mathbf{a}_{\rm BS}(\theta) = \mathbf{a}(\theta)$. In this case, the communication function has some theoretical limitations on the achievable data rate and the BER performance as given below.

1) Achievable Bit Rate: Given that the radar transmits one symbol per pulse, the symbol rate of the communication system is identical to the pulse repetition frequency ($f_{\rm PRF}$). The number of bits that can be transmitted per symbol is determined by the total number of unique symbols (or permutations), L, that are used

$$N_b = \lfloor \log_2(L_{\rm perm}) \rfloor, \tag{24}$$

where $\lfloor\cdot\rfloor$ denotes the floor function. The resulting bit rate of the system is $N_b \times f_{\rm PRF}$. In general, $L_{\rm perm}$ is not a power of 2 and the required number of symbols to transmit the N_b bits is

$$L = 2^{\lfloor \log_2(L_{\rm perm}) \rfloor} \leq L_{\rm perm}. \tag{25}$$

The fact that only a subset of the available symbols is required offers flexibility in the design of the actual system as well as providing improved noise immunity. However, a comprehensive

study of this task is beyond the scope of this work. In order to illustrate the performance of the proposed strategy, we employ enumeration (for relatively small M) to select the subset of L_{perm} symbols with inter-symbol distances $\|\mathbf{s}_{\ell'} - \mathbf{s}_{\ell}\|^2,\ \ell', \ell = 1, \ldots, L$.

The maximum achievable bit rate can be calculated in terms of the number of transmit elements as

$$N_b = \lfloor \log_2(M!) \rfloor. \tag{26}$$

This can be rewritten as

$$N_b = \left\lfloor \sum_{k=1}^{M} \log_2 k \right\rfloor. \tag{27}$$

A useful measure of the system's capacity is the achievable bit rate per antenna, which is obtained as

$$N_{bitsperantenna} \ = \ \frac{1}{M} \left\lfloor \sum_{k=1}^{M} \log_2 k \right\rfloor. \tag{28}$$

Now since $\lim_{M\to\infty} \frac{\log M}{M} = 0$, we can find a useful approximation for the number of bits for large M. Replacing the sum by the integral, we have

$$\begin{aligned} \tilde{N}_{bitsperantenna} &= \int_1^T \frac{1}{T} \log_2 x dx \\ &= \frac{1}{T \log 2} \left[x \log x - x \right]_1^T \\ &= \frac{1}{T \log 2} \left(T \log T - T + 1 \right) \\ &= \log_2 T - \frac{1}{\log 2} + \frac{1}{T \log 2}. \end{aligned} \tag{29}$$

Therefore, the number of bits per antenna per pulse for large M is given by

$$N_{bitsperantenna} \approx \left\lfloor \log_2 M - \frac{1}{\log 2} \right\rfloor \approx \lfloor \log_2 M \rfloor. \tag{30}$$

And the number of bits per PRI is

$$N_{bitsperpulse} \approx \left\lfloor M \log_2 M - \frac{M}{\log 2} + \frac{1}{\log 2} \right\rfloor. \tag{31}$$

2) Angular Ambiguities: Since the elements of the dictionary $\mathbb{D}$ are permutations on the steering vector $\mathbf{a}(\theta_c)$, L_{perm} is a function of the number of unique elements of $\mathbf{a}(\theta_c)$. For $\theta_c = 0$, that is when the communication receiver is at broadside, all elements of $\mathbf{a}(\theta_c)$ are real and $\mathbb{D} = \{\mathbf{s}_1(0)\}$ has only one element. We refer to this as *the degenerate case or trivial ambiguity*, and no information can be embedded via shuffling the transmit waveforms. When $\theta_c > 0$ is

small, the phases of the elements of $\mathbf{a}(\theta_c)$ are equally spaced on the unit circle with phase difference $\varphi_c \triangleq 2\pi d \sin(\theta_c)$. As θ_c increases, the angle φ_c increases and we reach an angle θ_M for which we have the largest spread around the unit circle. At this point, the minimum phase difference between any two elements of $\mathbf{a}(\theta_M)$ reaches its maximum value. We refer to this case as the *maximal spread angle* for which we have $\varphi_c = 2\pi/M$. The corresponding spatial angle is given by

$$\theta_M = \sin^{-1}\left(\frac{1}{Md}\right). \tag{32}$$

For $\theta_c > \theta_M$, it is possible that two (or more) elements of $\mathbf{a}(\theta_c)$ assume the same value. This occurs when their phases are equal modulo 2π. The first non-trivial ambiguity happens when $(M-1)\varphi_1 = 2\pi$. Solving for θ_1 we obtain

$$\theta_1 = \sin^{-1}\left(\frac{1}{(M-1)d}\right). \tag{33}$$

In this case, only two elements of $\mathbf{a}(\theta_1)$ overlap, namely $\mathbf{a}_0(\theta_1) = 1$ and $\mathbf{a}_{M-1}(\theta_1) = e^{j2\pi}$ and the cardinality of $\mathbb{D}$ is $L_{\text{perm}} = (M-1)!$. In general, ambiguities result whenever $(M-n)\varphi = 2\pi$, which implies that $\varphi_n = \frac{2\pi}{M-n}$ for $n = 1 \ldots M-1$. Solving for the spatial angles, we have

$$\theta_n = \sin^{-1}\left(\frac{1}{(M-n)d}\right),\ n = 1 \ldots M-1. \tag{34}$$

Note that for all angles θ_c other than the points of ambiguity, all elements of $\mathbf{s}_\ell$ are distinct and $L_{\text{perm}} = M!$. Figure 2 shows angular ambiguities and bits per symbol that can be transmitted versus the spatial angle for a MIMO system with $M = 10$ and $d = 0.5$. The red curve in the top graph gives the minimum angular separation of the elements of the symbol vectors $\mathbf{s}_\ell$. As predicted by (32), the maximal spread angle is $11.54°$, whereas the first ambiguity occurs for $\theta_c = 12.84°$ in agreement with (33). The number of bits that can be transmitted per symbol is shown by the blue curve in the bottom graph in Fig. 2. The system is able to transmit a maximum of 21 bits/symbol except at the discrete set of angles described in (34), where for each angle, the number of bits is reduced depending on the number of elements with unique phases. It is important to note, however, that for angles where the minimum angular separation is small, the performance may be poor if the full number of bits is used. Therefore, it is advantageous to transmit at the maximal spread angle θ_M which guarantees the best performance at the maximum data rate. In the following section, we describe a scheme to mitigate the ambiguities and steer the performance of the maximal spread angle to any receiver spatial angle.

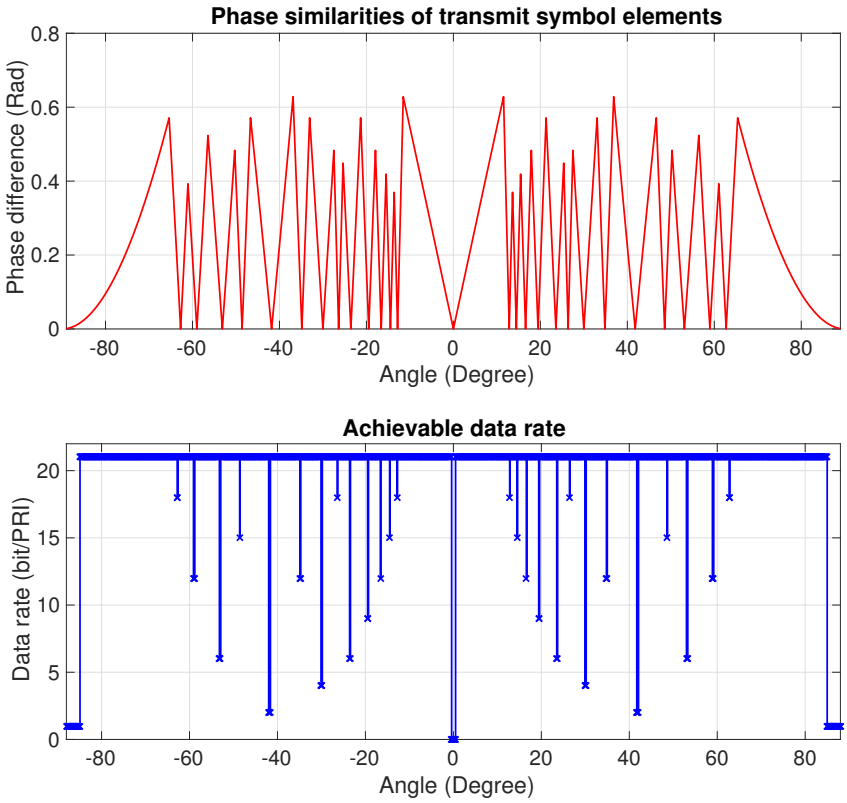

Fig. 2. System capacity as a function of the spatial angle of the communication receiver: (top) minimum angular separation between the symbol elements; (bottom) number of bits per symbol (number of bits per PRI) that can be transmitted.

3) Angular Ambiguity Mitigation: The ambiguities described above can be mitigated by inducing the required phases at the transmitter. Let us suppose we pre-multiply element-wise at the transmitter the vector of orthogonal waveforms, $\mathbf{\Psi}(t)$, by the vector $\mathbf{u} = [1\ e^{j\varphi}\ \ldots\ e^{j(M-1)\varphi}]$. Then, the vector of phase-shifted orthogonal waveforms becomes $\tilde{\mathbf{\Psi}}(t) = \mathbf{u} \odot \mathbf{\Psi}(t)$. Clearly, $\tilde{\mathbf{\Psi}}(t)$ still comprises orthogonal waveforms and the radar operations is unchanged. The matched-filtered signal at the communication receiver, however, becomes

$$\begin{aligned}\mathbf{r} &= \beta_{\text{ch}} \mathbf{P}_\ell^T \left(\mathbf{a}(\theta_c) \odot \mathbf{u}\right) + \mathbf{w} \\ &= \beta_{\text{ch}} \mathbf{s}^{(\ell)} + \mathbf{w}. \end{aligned} \tag{35}$$

The received symbol vector now has elements $\mathbf{s}_k^{(\ell)} = e^{jk(\varphi_c + \varphi)}$. Thus, we can induce a specific phase progression, φ_d, at the spatial angle θ_c of the communication receiver by setting $\varphi = \varphi_d - \varphi_c$. For example putting $\varphi_d = \varphi_M = \frac{2\pi}{M}$, we can induce the maximum angular spread at

any communication receiver θ_c. In this manner, not only are we able to mitigate the ambiguities, but also to deliver the best symbol dictionary to any receiver.

4) Symbol Error Rate: Let us assume without loss of generality that the transmitted symbol be $\mathbf{s}^{(i)}(\theta_c)$. Then, a symbol error occurs at the receiver whenever the noise places the received signal closer to another symbol, $\mathbf{s}^{(\ell)}(\theta_c)$, such that $\ell \neq i$. We now seek an upper bound for the probability, p_e, of symbol error. To this end, we proceed to write $p_e = 1 - P(\text{no error})$. Now let us define $d^{(\ell)} \triangleq \|\mathbf{r} - \mathbf{s}^{(\ell)}(\theta_c)\|^2$. Then, the probability of a correct symbol detection is given by

$$P(\text{no error}) = P\left(d^{(i)} < d^{(\ell)}, \forall\ \ell = 1 \ldots L, l \neq i\right). \tag{36}$$

Now for each symbol $\mathbf{s}^{(\ell)}(\theta_c)$, we have

$$\left\{d^{(i)} < d^{(\ell)}\right\} \supseteq \cap_{k=0}^{M-1} \left\{d_k^{(i)} < d_k^{(\ell)}\right\}. \tag{37}$$

Consequently, we have

$$P(d^{(i)} < d^{(\ell)}) \geq \prod_{k=0}^{M-1} P\left(d_k^{(i)} < d_k^{(\ell)}\right). \tag{38}$$

The problem on the right hand side is similar to a PSK scenario where the angular separation between two constellation points is given by $\gamma_k^{(i,\ell)} = \varphi^{(i)} - \varphi^{(\ell)}$. The possible values for γ_k are equal to $k\varphi_c$ for $m = 1, \ldots, (M-1)$. The probability of error can then be approximated at high SNR by $Q\left(\sqrt{2\rho}\sin\frac{\gamma_k}{2}\right)$, where $Q(x) = \frac{1}{2}\text{erfc}\left(\frac{x}{\sqrt{2}}\right)$ and erfc(x) is the standard complementary error function. Thus, we get

$$P\left(d_k^{(i)} < d_k^{(\ell)}\right) = 1 - Q\left(\sqrt{2\rho}\sin\frac{\gamma_k}{2}\right). \tag{39}$$

Clearly, an error may only occur if the two entries are not equal. Then, we arrive at

$$P(d^{(i)} < d^{(\ell)}) \leq \frac{1}{M}\sum_{k=0}^{M-1} P\left(d_k^{(i)} < d_k^{(\ell)} | \mathbf{s}^{(\ell)}(k)\right). \tag{40}$$

Since there are M elements, the upper bound on the probability of error becomes

$$P(\text{error}) \leq \left[\frac{1}{M}\sum_{k=0}^{M-1}\left(1 - Q\left(\sqrt{2\rho}\sin\frac{\gamma_k}{2}\right)\right)\right]^M. \tag{41}$$

B. MIMO Radar with K transmit Beams

The use of MIMO radar with transmit beams offers some advantages over the use of conventional MIMO radar with omnidirectional transmission. The first advantage is the increased SNR at the communication receiver due to the transmit processing gain associated with each transmit

beam. The second advantage is the ability to increase the bit rate per PRI by choosing the number of beams K to be larger than the number of elements M. In fact, according to [33], the number of transmit beams that can be achieved with the same transmit radiation pattern equals 2^{M-1}. Therefore, the bit rate that can be achieved is proportional to $\log_2(K!) = \log_2(2^{M-1}!)$. However, implementing this high limit of bit rate comes at the price of decreased detection efficiency due to the decreased phase separation $2\pi/K$.

As an illustrative example, assume that the number of transmit beams is chosen to be twice the number of transmit antennas, i.e., $K = 2M$. Then, the achievable bit rate per PRI can be found using Eq. (31) as

$$\begin{aligned} N_b &= \lfloor K \log_2 K \rfloor \\ &\approx \left\lfloor K \log_2 K - \frac{K}{\log 2} + \frac{1}{\log 2} \right\rfloor \\ &= \left\lfloor 2M \log_2 2M - \frac{2M}{\log 2} + \frac{1}{\log 2} \right\rfloor \\ &= 2 \left\lfloor M \log_2 2M - \frac{M}{\log 2} + \frac{1}{2 \log 2} \right\rfloor \\ &\geq 2N_{bitsperpulse}. \end{aligned} \tag{42}$$

Therefore, the use of a number of beams that is twice the number of antennas increases the achievable data rate by more than a factor of two. For example, if conventional MIMO radar is used with $M = 10$ elements, the maximum achievable bit rate is 21 bits per PRI while the use of $K = 20$ beams enables achieving a maximum data rate of $\lfloor (20!) \rfloor = 44 > 2(21)$ bits per PRI.

VI. Simulation Results

In order to demonstrate the capacity of the proposed system for establishing joint MIMO radar and communication operation, we consider a MIMO radar with a dual-function transmit platform comprising $M = 10$ omnidirectional transmit antennas. The transmit elements are arranged in a uniform linear array shape with interelement spacing of half a wavelength. We evaluate the system by comparing the performance of MIMO radar with transmit beamforming using $K = 4, 8,$ and 16 transmit beams to the performance of conventional MIMO radar with omnidirectional transmission. Throughout the simulations, we assume that the communication receiver is located in direction $\theta_c = -14^\circ$ and an eavesdropper is located in direction $\theta_e = 7^\circ$.

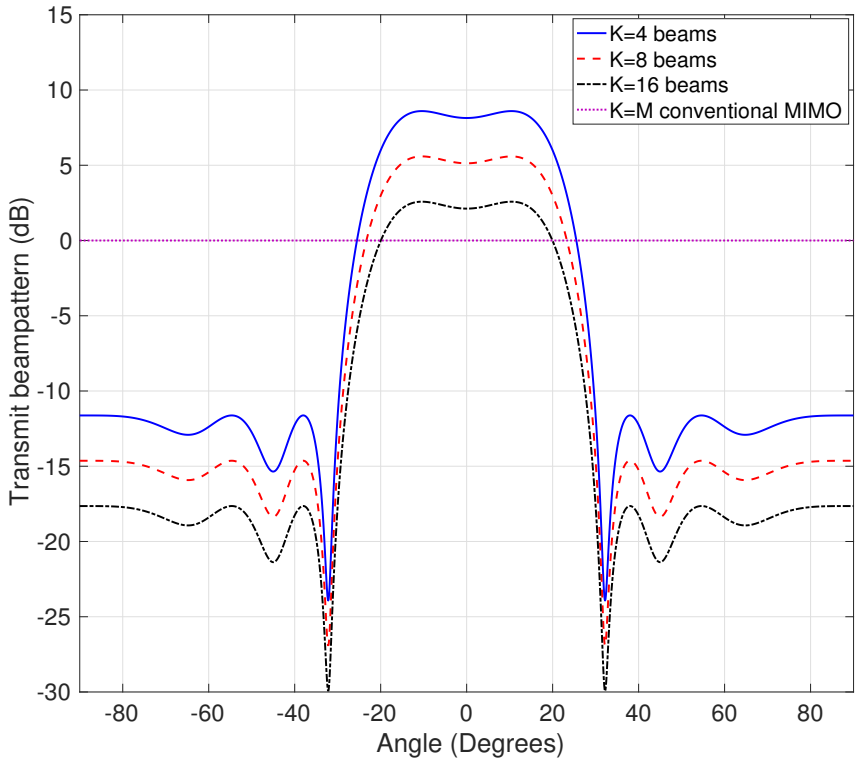

Fig. 3. Transmit beampattern versus angle for different numbers of transmit beams as well as for the case of conventional MIMO radar with omnidirectional transmission.

Example 1: Transmit beamforming Design for Joint Radar-communications

In the first example, we test the transmit beamforming design for joint radar-communications. We demonstrate the performance by showing the transmit beampattern versus angle, the transmit processing gain within the desired spatial sector for the MIMO radar operation, and the phase distribution of the formed communication symbols towards the intended communication direction. We assume that the general directions of the radar targets are located within the spatial sector $\Theta = [-15^\circ,\ 15^\circ]$. The radar operation requires focusing the transmit power within the sector Θ while keeping the sidelobe levels below a certain level, e.g., 20 dB below the main beam. We use the minmax criterion to design a principal weight vector that satisfies the radar requirements. Then, we employ the transmit radiation pattern invariance technique [33] to design 16 weight vectors which have the same radiation pattern as that of the principle weight vector but different phase value towards the intended communication direction. Each of the 16 weight

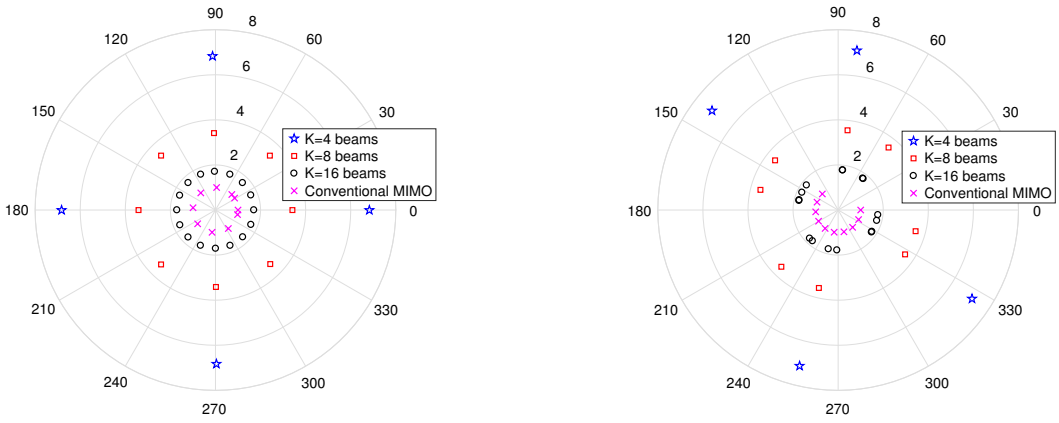

(a) (b)

Fig. 4. Communication symbol phase distribution for different values of K (a) phase versus gain of transmit beams towards the intended communication direction, i.e., distribution of $\angle\{\mathbf{W}^H\mathbf{a}(\theta_c)\}$ versus $\left|\mathbf{W}^H\mathbf{a}(\theta_c)\right|$ (b) phase versus gain of transmit beams towards the direction of the eavesdropper, i.e., distribution of $\angle\{\mathbf{W}^H\mathbf{a}(\theta_e)\}$ versus $\left|\mathbf{W}^H\mathbf{a}(\theta_e)\right|$

vectors is used to form a transmit beam. We consider three cases of MIMO radar with transmit beamforming $K = 4$, 8, and 16 transmit beams in addition to the case of conventional MIMO radar. For the two cases of $K = 4$ and 8 beams, two subsets of 4 and 8 transmit weight vectors are selected from the larger set of 16 weight vectors. For each case, the transmit beamforming matrix $\mathbf{W}$ is scaled such that the total transmit power is fixed to $\mathrm{trace}\{\mathbf{W}^H\mathbf{W}\} = 10$. Figure 3 displays the transmit beampatterns versus angle for all cases considered. The results demonstrate that the case of $K = 4$ beams has the highest transmit processing gain within the main beam since the total power is equally divided between the 4 beams. Note that the 4 beampatterns associated with the case of $K = 4$ are exactly the same; shown by blue color curve in the figure. As the number of beams increases, the transmit gain decreases as a result of dividing the transmit power among more beams. The figure also shows that the case of K =16 beams has higher gain within the main beam region than the conventional MIMO case which has a flat beampattern over the entire spatial domain.

The achievable bit rate per PRI depends on the number of distinct entries of the symbol $\mathbf{s}_\ell$ and the symbol detection performance depends on the separation between the corresponding phases as discussed in Sec. V. Figure 4 shows the distribution of the phase of each transmit beam versus the transmit gain for different values of K as well as for the case of conventional

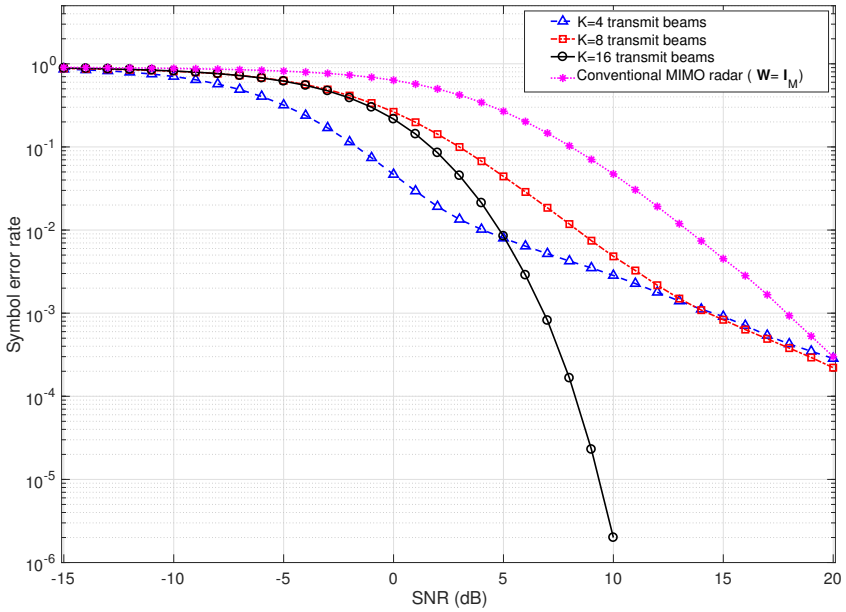

Fig. 5. SER versus SNR for the case where the communication receiver is at direction $\theta_c = -14^\circ$.

MIMO, i.e., for the case of $K = M$ and $\mathbf{W} = \mathbf{I}_M$. The phase distribution towards the intended communication direction is given in Fig 4-a, which shows that the phases associated with the cases $K = 4,\ 8$, and 16 are uniformly distributed within the $[0,\ 2\pi]$ interval. The figure also shows that the phases associated with the conventional MIMO case are not equally distributed within the $[0,\ 2\pi]$ interval. This can result in a reduced achievable bit rate per PRI and/or an increased symbol error rate. The phase distribution towards the eavesdropper is shown in Fig 4-b for all cases considered. The figure shows that all cases have distinct phases that are non-uniformly distributed within $[0,\ 2\pi]$. This means that the eavesdropper may still be able to detect the embedded information. In order to prevent the eavesdropper from intercepting the communication message, all phases (or at least some of the phases) towards the direction of the eavesdropper should be very close to each other. This case will be demonstrated in the last example in this section.

Example 2: Symbol Error Rate versus SNR

In the second example, we demonstrate the communication detection performance by showing the SER as a function of SNR. We use the same setup and the same number of beams used in

Example 1. The cases of $K = 4,\ 8,$ and 16 beams enable the embedding of the maximum bit rate of $N_b = 4,\ 15,$ and 44 bits per PRI, respectively, while the case of conventional MIMO radar enables the embedding of a maximum bit rate of 21 bits per PRI. However, in order to ensure a fair comparison, we fix the number of bits per PRI to $N_b = 4$. To implement that for the case of $K = 4$ beams, we generate a constellation of size $L = 16$ symbols that are selected from the total number of $L_{\text{perm}} = 4! = 24$ symbols. For the cases of 8 and 16 beams, the constellation comprises $L = 16$ symbols selected from the total number of $L_{\text{perm}} = 8!$ and $L_{\text{perm}} = 16!$, respectively. For the conventional MIMO case, the constellation consists of $L = 16$ symbols selected from the total number of $L_{\text{perm}} = 10!$. For the latter three cases, the total number of permutations is very large. Thus, for the purpose of this simulation the constellation is formed using $L = 16$ symbols that are selected randomly. In practice, however, the selection process may be optimized such that the symbol error rate is minimized. The optimization of constellation selection is outside the scope of this work. To demonstrate the symbol error rate performance, a number of 10^6 symbols are randomly generated from the set of integers $\{0, 1, \ldots, 15\}$. The communication receiver is assumed to be equipped with a single receive antenna. The complex channel coefficient is selected such that it has magnitude of unity and its phase is drawn randomly and uniformly from the set $[0,\ 2\pi]$. Figure 5 shows the SER versus SNR for $\theta_c = -14^\circ$. The SER curves exhibit the expected standard behavior of a communication system, with the bit error rate increasing with decreasing SNR. The results reveal that the use of MIMO radar with transmit beamforming outperforms the conventional MIMO radar case which can be attributed to the increased SNR at the communication receiver due to the coherent processing gain achieved through transmit beamforming. However, it can be seen from the figure that for low SNR values, the case of $K = 4$ beams has the best performance because it has the highest transmit gain. At high SNR values, the case of $K = 16$ beams has the lowest symbol error rate which can be attributed to the increased dimensionality of the symbol size and, correspondingly, the ability to choose a constellation of symbols that are as dissimilar from each other as possible.

Example 3: Information Embedding with Robustness against Eavesdropping

In the third example, we demonstrate the joint radar-communication performance with robustness against eavesdropping. We focus on the case of MIMO radar with $K = 16$ transmit beams and conventional MIMO radar. To achieve maximum communication performance, the transmit beamforming weight matrix $\mathbf{W}$ is designed such that the condition given in Eq. (22)

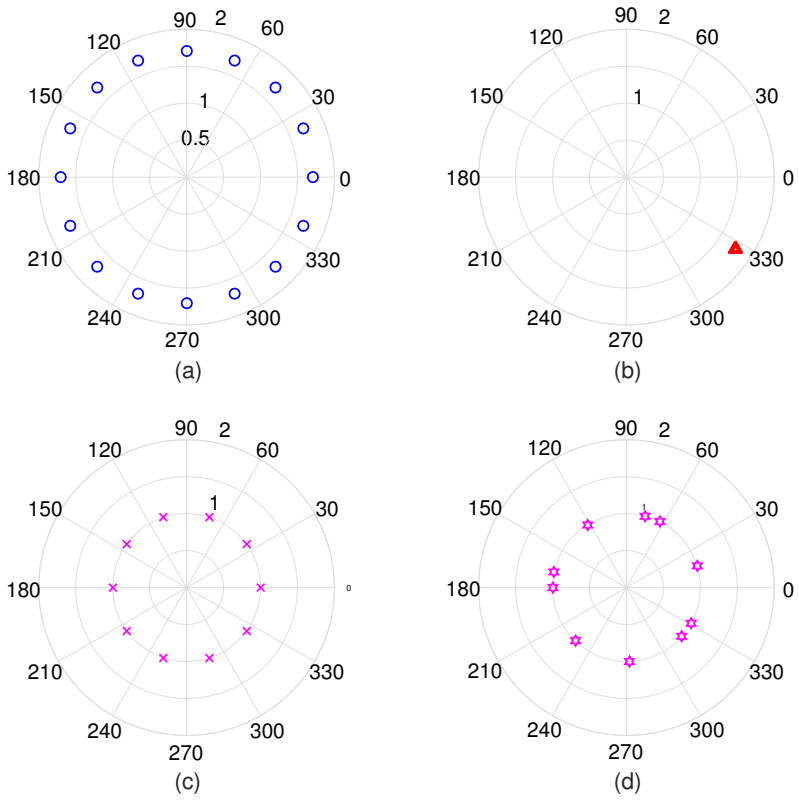

Fig. 6. Communication symbol phase distribution for MIMO radar with transmit beamforming using $K = 16$ beams and conventional MIMO radar with omnidirectional transmission (a) phase versus gain of $K = 16$ transmit beams towards the intended communication direction, i.e., distribution of $\angle\{\mathbf{W}^H\mathbf{a}(\theta_c)\}$ versus $\left|\mathbf{W}^H\mathbf{a}(\theta_c)\right|$ (b) phase versus gain of transmit $K = 16$ beams towards the direction of the eavesdropper, i.e., distribution of $\angle\{\mathbf{W}^H\mathbf{a}(\theta_e)\}$ versus $\left|\mathbf{W}^H\mathbf{a}(\theta_e)\right|$ (c) phase versus gain of conventional MIMO towards the intended communication direction, i.e., distribution of $\angle\{\mathbf{a}(\theta_c)\}$ on the unit circle (d) phase versus gain of conventional MIMO towards the direction of the eavesdropper, i.e., distribution of $\angle\{\mathbf{a}(\theta_e)\}$ on the unit circle

is satisfied, i.e., the phases $\angle\{\mathbf{W}^H\mathbf{a}(\theta_c)\}$ towards the intended communication direction are equispaced within the interval $[0,\ 2\pi]$ with separation $2\pi/16$ as shown in Fig. 6-a. On the other hand, to achieve robustness against eavesdropping the matrix $\mathbf{W}$ should satisfy the condition given in Eq. 23, i.e., the phases $\angle\{\mathbf{W}^H\mathbf{a}(\theta_e)\}$ towards the eavesdropper should be the same as shown in Fig. 6-b. For the conventional MIMO radar case, to achieve maximum communication detection performance we introduce phase ambiguity mitigation as explained in part 3) of Sec. V-A. This makes the phase distribution towards the intended communication direction uniform on the unit circle as shown in Fig. 6-c. However, choosing to mitigate phase ambiguity such that

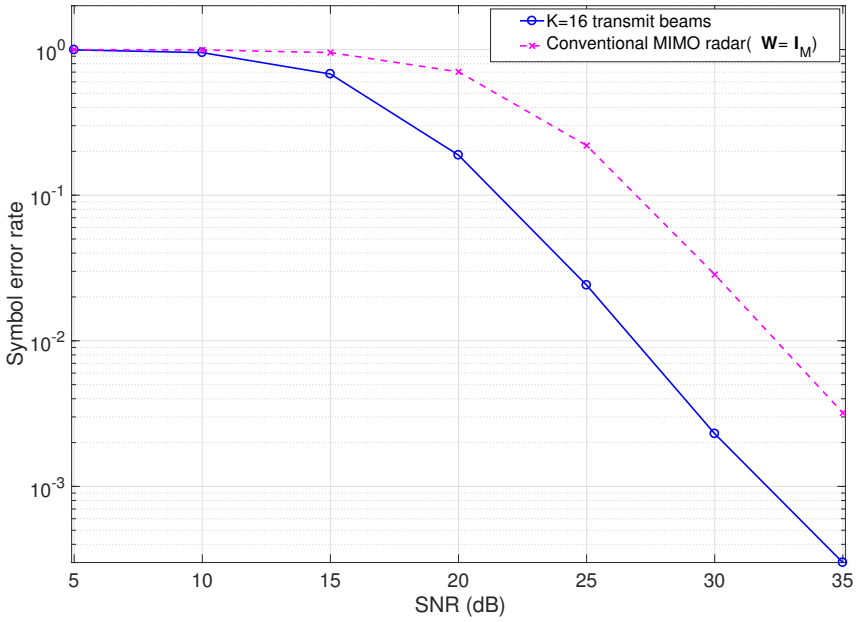

Fig. 7. SER versus SNR with the communication symbols constructed with phase distribution as in Fig. 6.

the communication detection is maximized does not guarantee that the eavesdropper will not be able to intercept the embedded information. This can be seen in Fig. 6-d where the phases towards the eavesdroppers are distinct and unique which enables detecting the message by the eavesdropper.

To demonstrate the SER performance versus SNR, we fix the bit rate per PRI to $N_b = 16$ for both methods. For the case of MIMO radar with $K = 16$ beams, a constellation of size $L = 2^{16} = 65536$ symbols are selected from the total number of $L_{\text{perm}} = 16!$. For the conventional MIMO case, a constellation of size $L = 2^{16} = 65536$ symbols are selected from the total number of $L_{\text{perm}} = 10!$. In both cases, the required constellations are selected randomly from the available permutations. Figure 7 shows the SER versus SNR for the two cases considered. The results demonstrate that the MIMO radar with 16 transmit beams outperforms the conventional MIMO radar.

The performance as a function of the receiver spatial angle for fixed SNR=30 dB is shown in Fig. 8. We display performance curves for 16 bits per symbol. The figure shows the SER performance for case of the MIMO radar with 16 transmit beams and the conventional MIMO radar. As expected, the communication system employing the MIMO radar with 16 transmit

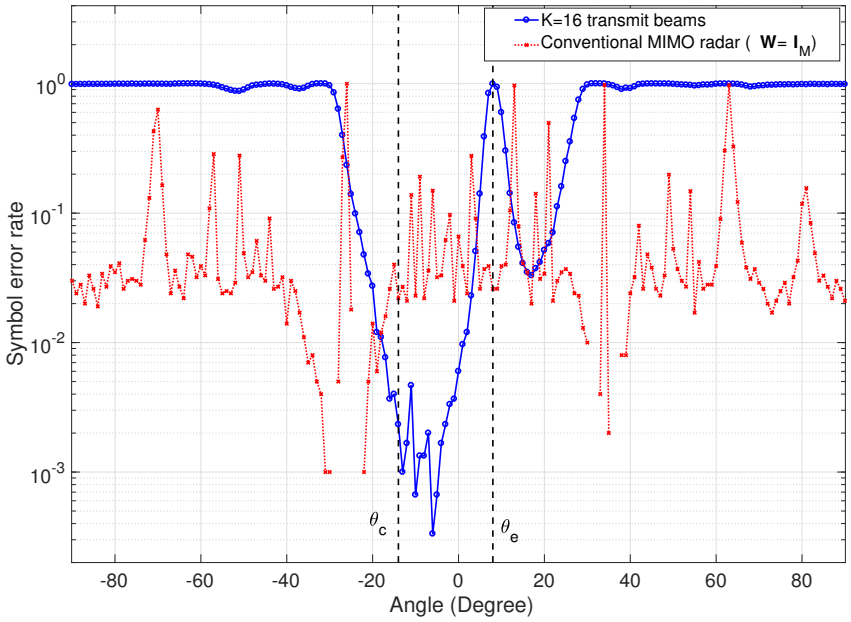

Fig. 8. SER versus spatial angle of the communication receiver with induced phases employed at the transmitter to shift the best performance towards $\theta_c = -14$. The SNR employed is 30 dB.

beams has lower SER towards the communication direction and maximum SER towards the eavesdropper at direction $\theta_e = 8°$. In addition, it prevents the message from being intercepted by any receiver located in the sidelobe region. On the other hand, the conventional MIMO radar curve exhibits low SER towards the intended communication direction but fails to prevent the eavesdropper at direction $\theta_e = 8°$ from intercepting the data. Moreover, the conventional MIMO exhibits fluctuating performance allover the spatial domain which agrees with the theoretical performance shown in Fig. 2.

VII. Conclusions

The problem of dual-function cooperative radar-communication system design was considered and a new technique for information embedding specific to MIMO radar was introduced. It was assumed that the system transmitter is either mounted on a stationary platform or its airborne spatial coordinate is provided to the communication receiver. In either case, the relative angle of the communication receiver to the radar transmitter is assumed known. The proposed technique exploits the fact that the MIMO radar receiver requires the knowledge of transmit waveforms-transmit antennas pairing, and does not require pinning a specific waveform to

a specific antenna. The flexibility of varying the waveforms across K transmit beams over different pulse repetition periods can be exploited to embed a large constellation of $K!$ symbols. This allows the transmission of $\lfloor \log_2(K!) \rfloor$ bits per PRI. The probability of error was analyzed and the bounds on the symbol error rate were derived. Simulation examples demonstrated the effectiveness of the proposed information embedding technique.

REFERENCES

[1] H. Griffiths, S. Blunt, L. Cohen, and L. Savy, "Challenge problems in spectrum engineering and waveform diversity," in *Proc. IEEE Radar Conf.*, Ottawa, Canada, April 2013, pp. 1–5.

[2] R. A. Romero and K. D. Shepherd, "Friendly spectrally shaped radar waveform with legacy communication systems for shared access and spectrum management," *IEEE Access*, vol. 3, pp. 1541–1554, 2015.

[3] H. Griffiths, L. Cohen, S. Watts, E. Mokole, C. Baker, M. Wicks, and S. Blunt, "Radar spectrum engineering and management: Technical and regulatory issues," *Proceedings of the IEEE*, vol. 103, no. 1, pp. 85–102, Jan 2015.

[4] J. R. Guerci, R. M. Guerci, A. Lackpour, and D. Moskowitz, "Joint design and operation of shared spectrum access for radar and communications," in *Proc. IEEE Radar Conf.*, Arlington, VA, May 2015, pp. 0761–0766.

[5] F. Liu, C. Masouros, A. Li, and T. Ratnarajah, "Robust MIMO beamforming for cellular and radar coexistence," *IEEE Wireless Communications Letters*, vol. 6, no. 3, pp. 374–377, June 2017.

[6] L. Wang, J. McGeehan, C. Williams, and A. Doufexi, "Application of cooperative sensing in radar–communications coexistence," *IET communications*, vol. 2, no. 6, pp. 856–868, 2008.

[7] D. W. Bliss, "Cooperative radar and communications signaling: The estimation and information theory odd couple," in *Proc. IEEE Radar Conf.*, Cincinnati, OH, May 2014, pp. 0050–0055.

[8] A. Aubry, A. D. Maio, Y. Huang, M. Piezzo, and A. Farina, "A new radar waveform design algorithm with improved feasibility for spectral coexistence," *IEEE Trans. Aerospace and Electronic Systems*, vol. 51, no. 2, pp. 1029–1038, April 2015.

[9] K.-W. Huang, M. Bica, U. Mitra, and V. Koivunen, "Radar waveform design in spectrum sharing environment: Coexistence and cognition," in *Proc. IEEE Radar Conf.*, Arlington, VA, May 2015, pp. 1698–1703.

[10] D. Ciuonzo, A. D. Maio, G. Foglia, and M. Piezzo, "Intrapulse radar-embedded communications via multiobjective optimization," *IEEE Trans. Aerospace and Electronic Systems*, vol. 51, no. 4, pp. 2960–2974, Oct 2015.

[11] B. Li, A. P. Petropulu, and W. Trappe, "Optimum co-design for spectrum sharing between matrix completion based MIMO radars and a MIMO communication system," *IEEE Trans. Signal Processing*, vol. 64, no. 17, pp. 4562–4575, Sept 2016.

[12] M. Bica and V. Koivunen, "Delay estimation method for coexisting radar and wireless communication systems," in *Proc. IEEE Radar Conference*, Seattle, WA, 2017, pp. 1557–1561.

[13] A. Martone, K. Ranney, K. Sherbondy, K. Gallagher, and S. Blunt, "Spectrum allocation for non-cooperative radar coexistence," *IEEE Transactions on Aerospace and Electronic Systems*, 2017.

[14] A. Hassanien, M. G. Amin, Y. D. Zhang, and F. Ahmad, "Signaling strategies for dual-function radar communications: an overview," *IEEE Aerospace and Electronic Systems Magazine*, vol. 31, no. 10, pp. 36–45, October 2016.

[15] A. Hassanien, B. Himed, and M. G. Amin, "Dual-function radar-communications using sidelobe control," in *Radar & Communication Spectrum Sharing*, S. D. Blunt and E. S. Perrins, Eds. IET, 2018.

[16] S. D. Blunt, M. R. Cook, and J. Stiles, "Embedding information into radar emissions via waveform implementation," in *Proc. IEEE Int. Waveform Diversity and Design Conf.*, Niagara Falls, Canada, 2010, pp. 195–199.

[17] J. Euziere, R. Guinvarc'h, M. Lesturgie, B. Uguen, and R. Gillard, "Dual function radar communication time-modulated array," in *Proc. IEEE Int. Radar Conf.*, Lille, France, 2014, pp. 1–4.

[18] A. Hassanien, M. G. Amin, Y. D. Zhang, and F. Ahmad, "A dual function radar-communications system using sidelobe control and waveform diversity," in *Proc. IEEE Radar Conf.*, Arlington, VA, May 2015, pp. 1260–1263.

[19] ——, "Dual-function radar-communications using phase-rotational invariance," in *European Signal Processing Conference*, Nice, France, 2015, pp. 1346–1350.

[20] M. Nowak, M. Wicks, Z. Zhang, and Z. Wu, "Co-designed radar-communication using linear frequency modulation waveform," *IEEE Aerospace and Electronic Systems Magazine*, vol. 31, no. 10, pp. 28–35, October 2016.

[21] A. Hassanien, M. G. Amin, Y. D. Zhang, and F. Ahmad, "Phase-modulation based dual-function radar-communications," *IET Radar, Sonar Navigation*, vol. 10, no. 8, pp. 1411–1421, 2016.

[22] A. Hassanien, B. Himed, and B. D. Rigling, "A dual-function MIMO radar-communications system using frequency-hopping waveforms," in *Proc. IEEE Radar Conf.*, Seattle, WA, May 2017, pp. 1721–1725.

[23] A. Hassanien, B. Himed, and M. G. Amin, "Transmit/receive beamforming design for joint radar and communication systems," in *Proc. IEEE Radar Conf.*, Oklahoma City, OK, April 2018.

[24] A. Hassanien, M. G. Amin, Y. D. Zhang, and F. Ahmad, "Dual-function radar-communications: Information embedding using sidelobe control and waveform diversity," *IEEE Trans. Signal Processing*, vol. 64, no. 8, pp. 2168–2181, April 2016.

[25] P. M. McCormick, S. D. Blunt, and J. G. Metcalf, "Simultaneous radar and communications emissions from a common aperture, part I: Theory," in *Proc. IEEE Radar Conf.*, Seattle, WA, May 2017, pp. 1685–1690.

[26] A. Hassanien, M. G. Amin, Y. D. Zhang, and B. Himed, "A dual-function MIMO radar-communications system using PSK modulation," in *European Signal Processing Conf.*, Budapest, Hungary, Aug 2016, pp. 1613–1617.

[27] E. BouDaher, A. Hassanien, E. Aboutanios, and M. G. Amin, "Towards a dual-function MIMO radar-communication system," in *Proc. IEEE Radar Conf.*, Philadelphia, PA, May 2016, pp. 1–6.

[28] A. Hunt, R. A. Romero, and Z. Staples, "The effect of embedded intrapulse communications on pulsed radar probability of detection," in *Proc. IEEE Global Conf. Signal and Information Processing (GlobalSIP)*, Montreal, QC, Canada, Nov. 2017, pp. 348–352.

[29] J. Li and P. Stoica, *MIMO radar signal processing*. John Wiley & Sons, 2008.

[30] M. Skolnik, *Introduction to Radar Systems*, 3rd ed. McGraw Hill, 2001.

[31] L. L. Monte, B. Himed, T. Corigliano, and C. J. Baker, "Performance analysis of time division and code division waveforms in co-located MIMO," in *Proc. IEEE Radar Conf.*, Arlington, VA, 2015, pp. 0794–0798.

[32] S. D. Blunt and E. L. Mokole, "Overview of radar waveform diversity," *IEEE Aerospace and Electronic Systems Magazine*, vol. 31, no. 11, pp. 2–42, November 2016.

[33] A. Hassanien, S. A. Vorobyov, and A. Khabbazibasmenj, "Transmit radiation pattern invariance in MIMO radar with application to DOA estimation," *IEEE Signal Processing Letters*, vol. 22, no. 10, pp. 1609–1613, Oct 2015.